A Hybrid QM−MM Potential Employing Hartree−Fock or Density Functional Methods in the Quantum Region

Paul D. Lyne,[†,‡] Milan Hodoscek,[§] and Martin Karplus*[,†,||]

Department of Chemistry and Chemical Biology, Harvard University, 12 Oxford Street, Cambridge, Massachusetts 02138, Physical and Theoretical Chemistry Laboratory, Oxford University, South Parks Road, Oxford OX1 3QZ, U.K., National Institute of Chemistry, Ljubjana, Hajdrihova 19, Slovenia, and Laboratoire de Chimie Biophysique, Institut le Bel, Université Louis Pasteur, 4, Rue Blaise Pascal, 67000 Strasbourg, France

Received: May 5, 1998; In Final Form: January 7, 1999

A hybrid quantum mechanical−molecular mechanical (QM−MM) potential energy function with ab initio and density functional capabilities has been implemented in the CHARMM program. It makes use of the quantum mechanical program CADPAC and the CHARMM molecular mechanics energy function; a GAMESS(US) interface to the CHARMM program was already available. To test the methodology, a series of relatively small systems are studied and comparisons are made of full QM calculations with those from various QM−MM partitions. Both density functional and Hartree−Fock calculations for the quantum region are presented and, where possible, compared with results from previous AM1−MM calculations. For the density functional based QM−MM calculations, the LDA and BLYP functionals were used. The performances of both the density functional and Hartree−Fock based QM−MM calculations compare well with pure quantum calculations. The link atom method was tested by performing a number of QM−MM simulations on the complexes of metal cations with model ligands of biological interest. It was found that it gave good results for the structures, binding energies, and charge distributions.

I. Introduction

The study of chemical reactions in condensed phases is one of the major challenges in computational chemistry. The difficulty arises from the need to simulate the system to a high degree of quantitative accuracy at an affordable cost. To simulate electronic states and charge redistribution, a quantum mechanical treatment is required.[1−3] The computational expense associated with high level quantum mechanical calculations imposes a severe restriction on the size of the system that can be studied.[4]

The emergence of hybrid quantum mechanical−molecular mechanical (QM−MM) methods in recent years addresses this problem. Pioneering studies of this type were made by Warshel and Levitt[5] and Singh and Kollman.[6] The method entails the division of the system of interest into a small region that is treated quantum mechanically, with the remainder of the system treated with computationally less expensive classical methods. The quantum region includes all the atoms that are directly involved in the chemical reaction being studied, and the remainder of the system, believed to change little during the reaction, is treated with a molecular mechanics force field.[7] The atoms in each system influence the other system through a coupled potential that involves electrostatic and van der Waals interactions.[6,8−18]

Several molecular mechanics programs have been adapted to perform hybrid QM−MM simulations. In the majority of the implementations the quantum region has been treated either by empirical valence bond methods[16] or with a semiempirical method (usually AM1).[19] These implementations have been applied, for example, to study solvation,[10,20] condensed phase spectroscopy,[21] conformational flexibility,[22] and chemical reactivity in solution,[23] in enzymes,[17,18,24,25] and in DNA.[26]

Although semiempirical methods have the advantage of being computationally inexpensive, they have a number of limitations.[27−30] The major limitations concern the accuracy and reliability of these methods. In general, they are less accurate than high-level ab initio methods, and since they have been parametrized to reproduce the ground-state properties of molecules, they are often not well suited to studying chemical reactions. A further disadvantage of the semiempirical methods is the limited range of elements for which parameters have been determined.

To overcome these limitations, the hybrid QM−MM potential can employ ab initio[2] or density functional methods[3] in the quantum region. Both of these methods can ensure a higher quantitative accuracy and the density functional methods offer a computationally less expensive procedure for including electron correlation.[4] Several groups have reported the development of QM−MM programs that employ ab initio[6,14,31] or density functional methods.[13,31,32]

The present paper reports the implementation and application of a QM−MM method for studying condensed phase systems, with the ability to use ab initio (HF), and density functional (DF) methods for the quantum region. The original AM1−MM method of Field et al.[8] has served as a model for the HF−MM or DF−MM implementations. Many authors have repeated the studies of simple ion−water complexes presented in Field et al.[8] as tests of hybrid QM−MM potentials. As a first test of the implementation, we studied some of the same ion−water

[†] Harvard University.
[‡] Oxford University.
[§] National Institute of Chemistry.
[||] Université Louis Pasteur.

10.1021/jp982115j CCC: $18.00
Published on Web 04/15/1999

complexes to compare the results with the AM1−MM method and various other HF−MM and DF−MM methods. To illustrate the advantage of the ab initio and density functional methods over semiempirical based QM−MM methods, and as a preparation for studying chemical reactions in enzyme systems, we have performed additional test studies of models for biological ligands complexed with Mg^{2+} and Ca^{2+}. Since semiempirical methods only consider the valence electrons, these ions would be represented as point charges when treated in the quantum region by semiempirical based QM−MM methods. An issue that arises when performing QM−MM simulations of enzymes is the treatment of the boundary between the QM and MM regions that involve chemical bonds. Field et al. [8] employed "link" atoms to cap the quantum region when the QM−MM boundary lies across a bond. To assess the use of link atoms in HF−MM and DF−MM calculations, we have performed tests in which the QM−MM partition is made within a single molecule.

II. Methods

Hybrid Potential. The QM−MM potential energy function implemented here is conceptually similar to that developed by Field et al.[8] The total energy of the system is calculated by solving the Schrödinger equation with an effective Hamiltonian for the mixed quantum and classical system:

$$\hat{H}_{\text{eff}}\Psi(r,R_\alpha,R_M) = E(R_\alpha,R_M) \tag{1}$$

where Ψ is the electronic wave function of the quantum system. It depends directly on the electron coordinates r and parametrically on the coordinates of the quantum and classical nuclei; they are referred to as R_α and R_M, respectively.

The Hamiltonian can be partitioned into quantum and classical components[8] by writing

$$\hat{H}_{\text{eff}} = \hat{H}_{QM} + \hat{H}_{MM} + \hat{H}_{QM-MM} \tag{2}$$

where $\hat{H}_{QM}$ is the pure quantum Hamiltonian, $\hat{H}_{MM}$ is the classical Hamiltonian and $\hat{H}_{QM-MM}$ is the hybrid QM−MM Hamiltonian. Given eq 2, the total energy can be written

$$E(R_\alpha,R_M) = \frac{\langle\Psi|\hat{H}_{QM}|\Psi\rangle + \langle\Psi|\hat{H}_{QM-MM}|\Psi\rangle}{\langle\Psi|\Psi\rangle} + \text{EMM}$$
$$= E_{QM} + E_{QM-MM} + E_{MM} \tag{3}$$

For hybrid QM−MM calculations using density functional theory for the quantum region, the electronic energy terms (E_{DF} and E_{DF-MM}) explicitly depend on the electron density, $\rho(r)$, of the atoms in the quantum region.[3] The electron density is determined by solving self-consistently the one-electron Kohn−Sham equations:[3,33]

$$\hat{H}_{DF}\psi_i(r) = e_i\psi_i(r) \qquad i = 1, ..., n \tag{4}$$

where ψ_i is a one-electron wave function and e_i is the associated eigenvalue. The Hamiltonian $\hat{H}_{DF}$ is given by

$$\hat{H}_{DF} - \sum_i \frac{\hbar^2}{2m_i}\nabla_i^2 - \sum_{i\alpha}\frac{Z_\alpha}{r_{i\alpha}} - \sum_{iM}\frac{q_M}{r_{iM}} + \sum_{\alpha\beta}\frac{Z_\alpha Z_\beta}{R_{\alpha\beta}} + \int\frac{\rho(r')}{|r-r'|}dr' + \frac{\partial E_{XC}}{\partial\rho(r)} \tag{5}$$

In eq 5 $\rho(r)$ is the electron density ($\rho(r)\sum_i|\psi_i(r)^2|$ where the sum is over all occupied Kohn−Sham orbitals i), E_{XC} is the exchange correlation functional,[3] q_M is the net charge of an MM atom, Z_α is the nuclear charge of quantum atom α, $r_{i\alpha}$ is the distance between electron i and the quantum atom α, r_{iM} is the distance between electron i and the MM atom M and $R_{\alpha\beta}$ is the distance between quantum atoms α and β, and r' refers to the coordinates of a second electron. Once the eqs 4 have been solved for the Kohn−Sham orbitals ψ_i, the contributions in eq 3 are evaluated from the expressions

$$E_{DF} = -\frac{\hbar^2}{2m}\int\sum_i\psi_i(r)\nabla^2\psi_i(r)\,dr - \int\sum_\alpha\frac{Z_\alpha}{|r_\alpha - r|}\rho(r)\,dr + \frac{1}{2}\int\int\frac{\rho(r)\,\rho(r')}{|r-r'|}dr\,dr' + E_{XC}[\rho(r)] + \sum_\alpha\sum_{\beta>\alpha}\frac{Z_\alpha Z_\beta}{R_{\alpha\beta}} \tag{6}$$

and

$$E_{DF-MM} = -\int\sum_M\frac{q_M}{|r_M - r|}\rho(r)\,dr + \sum_{\alpha,M}\frac{q_M Z_\alpha}{R_{\alpha M}} + \sum_{\alpha,M}V_{\alpha M} \tag{7}$$

where $V_{\alpha M}$ is the van der Waals interaction energy between the quantum and classical regions and is described below. For ab initio Hartree−Fock based QM−MM calculations (HF−MM) the analogous equations for the electronic Hamiltonian and the corresponding energies are[1]

$$E = \frac{1}{2}\sum_\mu\sum_\nu P_{\mu\nu}(H_{\mu\nu}^{\text{core}} + F_{\mu\nu}) + \sum_\alpha\sum_{\beta>\alpha}\frac{Z_\alpha Z_\beta}{R_{\alpha\beta}} + \sum_{\alpha,M}\frac{q_M Z_\alpha}{R_{\alpha M}} + \sum_{\alpha,M}V_{\alpha M} \tag{8}$$

where $H_{\mu\nu}^{\text{core}}$ is defined as

$$H_{\mu\nu}^{\text{core}} = \int\phi_\mu^*\left[-\frac{1}{2}\nabla^2\right]\phi_\nu\,dr + \int\phi_\mu^*\left[-\left(\sum_\alpha\frac{Z_\alpha}{|R_\alpha - r|} + \sum_M\frac{q_M}{|R_M - r|}\right)\right]\phi_\nu\,dr \tag{9}$$

The indices μ and ν refer to the basis set orbitals ϕ, and $P_{\mu\nu}$ and $F_{\mu\nu}$ are elements of the density and Fock matrices.[1] The Lennard-Jones interaction energy, $V_{\alpha M}$, is common to both types of calculation and is given as

$$V_{\alpha M} = 4\epsilon_{\alpha M}\left[\left(\frac{\sigma_{\alpha M}}{R_{\alpha M}}\right)^{12} - \left(\frac{\sigma_{\alpha M}}{R_{\alpha M}}\right)^{6}\right] \tag{10}$$

where the sum over α is over all QM atoms and the sum over M is over all MM atoms. This term is essential to obtain the correct structure since there is no Pauli repulsion between QM and MM atoms.

The molecular mechanics energy contribution, E_{MM}, is calculated with the standard CHARMM potential energy functions.[34]

Computational Details. For the purposes of performing QM−MM calculations, interfaces were written in CHARMM[34] to incorporate the quantum mechanical packages CADPAC;[35] the GAMESS(US) program[36] had been interfaced with CHARMM by B. Brooks and M. Hodoscek (unpublished)[18].

Density functional calculations with CADPAC were performed in the local density approximation (LDA) level using the Vosko, Wilk, and Nusair parametrization[37] of Monte Carlo calculations by Ceperley and Alder[38] on a series of homogeneous electron gases. Nonlocal density functional calculations were performed using the nonlocal exchange correction of Becke[39] and the nonlocal correlation correction of Lee, Yang, and Parr,[40] as transformed by Miehlich et al.[41] (BLYP). The nonlocal corrections for the BLYP calculations were included self-consistently. Numerical integration was performed for the density functional calculations using numerical quadrature[42] with a MEDIUM sized grid, as defined in CADPAC. For the MM atoms, standard CHARMM22 parameters were used;[43] unlike some other QM−MM implementations,[44] no optimization of the van der Waals parameters for the interaction between QM and MM atoms was made. For the small systems studied nonbonded cutoffs were not employed in the calculations so that all interactions were included. The basis set used for each calculation is given in the appropriate table of results. The procedure for handling QM−MM boundaries across covalent bonds is to use a link atom to cap the quantum region.[8] The implementation of this approach is the same as that used in the semiempirical QM−MM method of Field et al.[8] except that the link atom is treated as a proper QM atom and, as such, feels the charges from the atoms in the MM region. The charges on the MM functional group or atom that is "replaced" by the link atom do not contribute to the one-electron integrals in the self-consistent calculation for the quantum region. For CH_3CH_2OH with OH treated by QM and CH_3CH_2 treated by MM as an example, the charges on the CH_2 group are not included in the QM Hamiltonian; all other MM charges (i.e., from the CH_3 group) are included. The link atom is initially positioned 1 Å along the original bond but is not constrained during optimization. The other classical energy terms included in the boundary region are the same as those described in detail by Field et al.[8]

III. Results and Discussion

As a first test, several of the complexes studied by Field et al.[8] with the AM1−MM potential have been treated. They are classified according to the total charge on the complex and whether link atoms were required. A comparison of the results from the previous AM1−MM studies and the HF−MM and DF−MM results was made. Also, the relative performance of the HF−MM and the various DF−MM calculations was assessed. Since the ability of the method to accurately model the interactions between a solute and solvent molecule is crucial to future condensed phase studies, almost all of the binary complexes include water.

The calculations were performed in the gas phase to allow comparison with pure quantum mechanical studies and available experimental data. For the purposes of clarity, specific results with the DF−MM method are referred to by the functional that was used; for example, a DF−MM calculation with the BLYP functional is referred to as BLYP−MM. The basis sets employed are described in the legends of the appropriate tables. All degrees of freedom were optimized using a conjugate gradient minimization method. The calculations are not corrected for basis set superposition error (BSSE). In the case of the cation water complexes this is expected to be in the range of 1−2 kcal/mol on the basis of previous studies.[45] For the larger complexes that employ link atoms, the BSSE for the QM and QM−MM calculations are expected to be very similar. An additional issue that arises in the comparison of QM and QM−MM results is the different treatment of dispersion interactions in the various methods. For the present cases the magnitude of the dispersion energy in the MM systems is small relative to the interaction energies, particularly for the complexes studied in the link atom tests.

TABLE 1: Binding Energy, Δ*E*, and Structural Data for the Water Dimer[a]

	Δ*E*	*d*(H···O)	*d*(O···O)	∠O···HO
	Hybrid Potential Calculations			
H_2O(donor)[b]				
HF−MM	7.389	1.761	2.738	178.4
LDA−MM	7.136	1.765	2.742	179.2
BLYP−MM	6.768	1.772	2.746	179.3
AM1−MM	3.300	2.150	2.944	159.5
H_2O(acceptor)[c]				
HF−MM	7.398	1.732	2.711	178.87
LDA−MM	7.139	1.736	2.715	179.37
BLYP−MM	6.749	1.746	2.723	179.52
AM1−MM	4.600	1.990	2.983	169.0
	Full Quantum Calculations			
HF	5.710	1.986	2.898	177.2
LDA	10.74	1.751	2.720	171.3
BLYP	6.320	1.921	2.882	174.1
	Full Classical Calculation			
CHARMM	7.075	1.749	2.726	176.3
experiment[d]	5.44 ± 0.7		2.98	174 ± 20

[a] The units of energy are kcal/mol; bond lenghts are in Ångstroms and bond angles in degrees. For the hybrid potential calculations the TIP3P model was used for the MM region and the 6-31G* basis set was used for the quantum region. Calculations were performed for the hydrogen bond donor in the quantum region and repeated for the donor in the classical region. All degrees of freedom were optimized. No counterpoise correction was used in the QM calculations. [b] H_2O(donor) corresponds to system I in Figure 1 in which the donor molecule is treated quantum mechanically. [c] H_2O(acceptor) corresponds to system II in Figure 1 in which the acceptor molecule is treated quantum mechanically. [c] See refs 42 and 43.

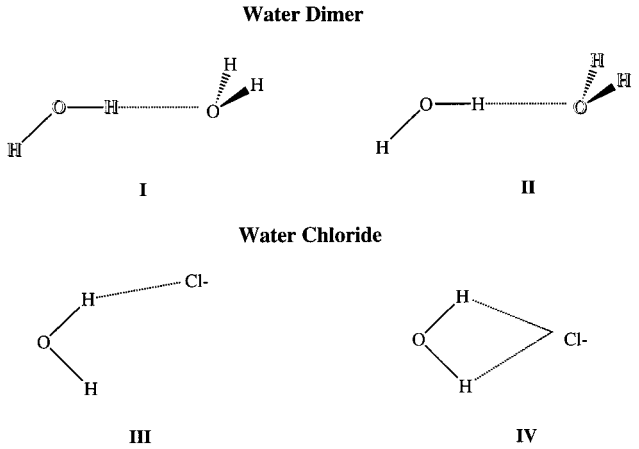

Figure 1. (I) Water dimer with the hydrogen bond donor in the quantum region. (II) Water dimer with the hydrogen bond acceptor in the quantum region. (III) The minimum energy structure for the complex of water with chloride. (IV) The saddle point for interconversion between different C_s isomers of the water−chloride complex.

Water Dimer. The water dimer is a standard test case for QM−MM methods.[8,11,31] The geometries and binding energies for the water dimer system calculated at the various levels of theory are presented in Table 1. Two possibilities for partitioning the system are considered, corresponding to whether the hydrogen bond donor is treated quantum mechanically or classically (see Figure 1). In considering the results, one should note that the MM water model (TIP3P[45,46]) includes the average polarization expected in liquid water; i.e., the dipole moment

TABLE 2: Binding Energy, Δ*E*, and Structural Data for the Water−Chloride Ion Dimer[a]

	Δ*E*	*d*(O···Cl⁻)	∠OH···Cl	*d*(H···Cl⁻)	*d*(H′···Cl⁻)	Δ*E*	*d*(O···Cl⁻)	∠OH···Cl	*d*(H···Cl⁻)	*d*(H′···Cl⁻)
Hybrid Potential Calculations										
	QM Water					MM Water				
HF−MM	15.29	3.130	163.5	2.187	3.245	14.16	3.238	134.6	2.478	2.936
LDA−MM	15.53	3.117	164.3	2.145	3.270	14.18	3.237	134.7	2.474	2.939
BLYP−MM	14.80	3.128	164.4	2.147	3.246	14.18	3.236	134.9	2.474	2.939
AM1−MM[b]	10.40	3.320	138.9	2.578	3.144	13.50	3.290	116.5	2.745	2.745
	Full Quantum Calculations									
HF	14.25	3.266	153.9	2.376	3.275					
LDA	22.10	3.020	161.8	2.044	3.073					
BLYP	15.98	3.161	157.8	2.203	3.230					
	Full Classical Calculation									
CHARMM	17.26	3.21	129.8	2.501	2.823					
experiment	13.4									

[a] The energy is in kcal/mol; bond lenghts are in Ångstroms, and bond angles are in degrees. For the hybrid potential calculations the TIP3P model was used for water in the MM region and the 6-31G* basis set for all quantum calculations. Calculations were performed for the water in the quantum region and repeated for water in the classical region. All degrees of freedom were optimized. No counterpoise correction was used in the QM calculations. [b] For the AM1−MM calculations the symmetry of the complex changes with the partition of the system. When water is in the quantum region, the complex has C_{2v} symmetry.

is larger than the gas-phase value so that the interaction energies would be expected to be overestimated.

The interaction energies from the QM−MM studies are somewhat higher than experiment for the HF−MM and DF−MM calculations, with the results from the QM donor system being slightly better than the QM acceptor results. The HF−MM and DF−MM results are closer to the experimental value than the AM1−MM result[8] for the QM donor, but AM1−MM is better for the QM acceptor model. More important is the fact that the QM−MM energies are much closer to those obtained from a full QM calculation in both cases.

There are large differences in the structural results obtained with the HF−MM and DF−MM studies relative to the AM1−MM calculations.[8] The AM1−MM method predicts a considerable deviation from linearity for the hydrogen bond angle, H···OH. The HF−MM and DF−MM calculations predict an almost linear hydrogen bond. These results are in agreement with high-level pure quantum mechanical studies of the water dimer[47] and the pure quantum results given in the table. The experimental error for the hydrogen bond angle[48,49] is too large to compare the theoretical and experimental results. The HF−MM and DF−MM calculations consistently underestimate the *d*(O···O) distances by approximately 0.2 Å compared with the pure quantum values.

Overall, the BLYP−MM method gives the best results for the energy of the water dimer calculations. The BLYP−MM results are better than those obtained with the HF−MM for this basis set (i.e., they agree better with the corresponding pure quantum result and with the experimental binding energy). The nonlocal DF−MM results are generally better than the LDA−MM results, though the LDA−MM calculations yield geometries that are slightly closer to the full QM calculations than the corresponding BLYP results. The performance of both HF−MM and DF−MM is much better than the AM1−MM method.[8]

Anion−Water Complexes. The complex between water and the chloride ion was difficult to model for the AM1−MM potential.[8] Many quantum mechanics studies[50,51] of this system have established that the minimum has C_s symmetry. Field et al.[8] found that treating the water as QM and the halide ion as MM gave the correct symmetry for the complex but that the opposite partitioning of the complex predicted a minimum with C_{2v} symmetry. The structure with C_{2v} symmetry is predicted by pure quantum mechanics calculations to be a transition state for the interchange of hydrogen bonds. The C_s and C_{2v} structures are depicted in Figure 1. The results for the HF−MM and DF−MM calculations for this complex are given in Table 2.

In contrast to the AM1−MM results both the HF−MM and DF−MM methods find that the minimum for this complex has C_s symmetry irrespective of the partitioning scheme. The calculated binding energies whether by QM or QM−MM are reasonably close to the gas-phase and to the experimental values[52] (except for AM1−MM with QM H_2O). The pure MM calculation gives a somewhat larger binding energy because of the use of a polarized water molecule (see above). The pure quantum results with LDA show an anomalously high binding energy (a characteristic flaw of LDA[53]). Interestingly, this binding energy is reduced in the LDA−MM calculation. The binding energies are consistently higher when the water is treated quantum mechanically, except for AM1−MM. The largest discrepancies in the binding energy occur for AM1−MM with QM water (3.4 kcal/mol) and for LDA−MM (2.1 kcal/mol) with QM water. When the chloride is in the quantum region, the largest discrepancy is only 1.1 kcal/mol, which occurs with the HF−MM method. These are satisfactory results considering that the pure quantum mechanical calculation with the same basis set overestimates the binding energy by 0.85 kcal/mol. The binding energies are better than those predicted[8] by AM1−MM, especially since the AM1−MM method did not predict the correct geometry for the complex. In the absence of experimental data, the geometries are compared with the results from pure quantum mechanical calculations. The bond distances are in very good agreement with pure quantum results. However, the QM−MM angles show greater deviations from the pure quantum mechanical results, with an underestimation of approximately 18° when the chloride is in the QM region. The DF−MM and HF−MM methods perform equally well for this complex.

Cation−Water Complexes. The important roles of metal ions in biological systems is well documented. Cation−water complexes involving Na^+ and Mg^{2+} were chosen for the first test; other systems are considered in section IV. In each case an all-electron treatment of the quantum region was made; this contrasts with the semiempirical QM−MM methods. In the latter case, metal ions such as Na^+ and Mg^{2+} are essentially treated as point charges by AM1 and PM3 since these methods only

TABLE 3: Binding Energy, ΔE, and Structural Data for the Na^+ and Mg^{2+} Complexes with Water[a]

	ΔE	d(O···M)	∠OH···M	ΔE	d(O···M)	∠OH···M
			Hybrid Potential Calculations			
		QM Water			MM Water	
Na^+						
HF−MM	30.50	2.153	127.7	28.05	2.190	130.1
LDA−MM	29.70	2.156	127.7	28.08	2.190	130.1
BLYP−MM	28.24	2.163	128.1	28.07	2.190	130.1
		Full Quantum Calculations				
HF	28.57	2.215	127.2			
LDA	34.41	2.118	127.1			
BLYP	30.86	2.168	127.4			
		Full Classical Calculation				
CHARMM	30.58	2.189	130.36			
experiment	24.0					
			Hybrid Potential Calculations			
		QM Water			MM Water	
Mg^{2+}						
HF−MM	85.40	2.037	127.6	79.46	1.962	132.8
LDA−MM	84.40	1.908	127.6	79.48	1.961	132.8
BLYP−MM	81.12	1.911	127.7	79.48	1.961	132.8
		Full Quantum Calculations				
HF	80.21	1.934	127.2			
LDA	96.71	1.923	126.8			
BLYP	91.75	1.954	126.9			
		Full Classical Calculation				
CHARMM	85.00	1.961	133.2			

[a] The units of energy are kcal mol^{-1} and the structural units are Ångstroms for bond lengths and degress for bond angles. For the hybrid potential calculations the TIP3P model was used for water in the MM region and the 6-31G* basis set was used for the quantum region. Calculations were performed for the water in the quantum region, and repeated for water in the classical region. All degrees of freedom were minimized. No counterpoise correction was used in the QM calculations.

consider valence electrons in the quantum calculation. In addition, it is not possible to study the Mg^{2+}/H_2O) system with AM1−MM methods since AM1 has not been parametrized for Mg^{2+}. Consequently, only HF and DFT based QM and QM−MM results are given in Table 3.

The ions and the water molecule were alternatively treated as quantum and classical systems in the QM−MM calculations. The results for the sodium ion and water are close to those obtained by the pure quantum calculations. The binding energies are slightly overestimated by the HF−MM and DF−MM methods for both partition schemes with respect to the experimental value, but both methods reproduce the pure quantum value quite well with the exception of LDA, which once again has a higher binding energy relative to the other pure quantum methods. The results for the geometries are very close to the pure quantum mechanics calculation, with slightly better agreement obtained for the case when water is treated by QM.

For the (Mg^{2+}/H_2O) complex, the quality of the calculated binding energies for the HF−MM and DF−MM calculations is not as good as for Na^+. When the water is in the quantum region, the binding energy is overestimated for the HF−MM method and underestimated for the DF−MM methods, relative to the QM results. When the magnesium ion is in the quantum region, the binding energy is consistently underestimated for the HF−MM method and the DF−MM methods. These are the poorest results obtained for all the systems considered in this study. A more realistic physical description of these systems should take account of polarization, which is absent from the current QM−MM method. Polarization effects can be included in the calculation through the introduction of an extra term in the effective Hamiltonian of eq 2.[54,55] This extra term, H_{pol}, is given by

$$H_{pol} - \frac{1}{2}\sum_{M}\sum_{\alpha}\frac{\mu_M^{ind}}{r_{\alpha M}^3}\mathbf{r}_{\alpha M} + \frac{1}{2}\sum_{M}\sum_{\alpha}\frac{Z_M\mu_M^{ind}}{R_{\alpha M}^3}\mathbf{R}_{M\alpha} \quad (11)$$

The induced dipole moment of the classical atoms, μ_M^{ind}, is directly coupled to the wave function of the quantum system, and so the polarization needs to be calculated self-consistently. It is feasible to perform this type of calculation for the small systems studied here, but the computational cost would be prohibitive for an enzyme, for example. Since the present test calculations have as their objective the HF−MM amd DF−MM treatment of reactions in proteins, which already is computationally intensive, we do not investigate polarization here. A possibility would be to consider a three-region system based on ab initio QM, semiempirical QM for polarization, and MM for the rest of the protein.

Any small ion, such as those considered in this study would be expected to polarize the water molecule to some extent. A strong polarization is expected to result from the interaction of the doubly charged magnesium with water, and this may explain the large discrepancy in the binding energy found for the Mg^{2+}/H_2O complex when the magnesium ion is in the quantum region and H_2O is in the MM region. This illustrates that care is required when partitioning a system that includes highly charged species such as Mg^{2+}. It is interesting in this regard that the CHARMM energy value, which was parametrized using ab initio data (Prodhom et al. unpublished) gives reasonable results. Ideally, the atoms directly coordinated to the metal should also be included in the quantum region. Unfortunately, this increases

the size of the quantum region. An alternative would be to reparametrize the MM atoms that coordinate to the metal or to introduce a local polarization term.[56] In other applications of the AM1−MM potential it was found that an optimization of the empirical van der Waals parameters of the QM and MM atoms is necessary to produce satisfactory results.[57]

IV. Link Atom Tests: Divalent Cations with Biological Ligand Analogues

In some systems it is desirable to partition different parts of the same molecule into quantum and classical regions. One case where this is essential is for an enzyme−substrate complex, where active site residues of the enzyme participate in the reaction. Since there is no exact procedure for introducing such a partitioning, a variety of approximate methods[8,14,58,59] have been used to deal with the truncation of the electron density that arises when the system is partitioned across a covalent bond. We employ the "link atom" approach, in which a hydrogen atom is used to complete the valency of the atom where the truncation occurs and is placed along the bond between the quantum and classical regions. This is analogous to an approach used to truncate the systems in pure QM calculations.[60,61] The link atom is part of the full quantum calculation, but it does not have a van der Waals interaction with the atoms in the MM region. The "link atom" method was used in the AM1−MM method of Field et al.,[8] and the HF−MM method of Singh and Kollman.[6] The approach used here is a modification of that presented by Field et al.,[8] as described in the "Computational Details" section.

For the AM1−MM method it is known from the work of Field et al.[8] that care must be taken when deciding where to partition a molecule into quantum and classical regions. In general, different partitioning should be investigated to verify that consistent results are obtained. Field et al.[8] advised against partitioning the system across π -bonds, or other bonds that are involved in conjugation. Also, if large charge shifts occur, the partitioning may have to be displaced.

In this section the results from simulations employing the QM−MM method with link atoms are presented. We investigate the interactions of divalent metal ions with model biological ligands. Examples where this is important is for metal-containing enzymes such as xylose isomerase[62] and for ribozymes.[63] The interactions of Mg^{2+} and Ca^{2+} with model ligands containing functional groups commonly found in biomolecules are reported. Acetate and propanoate were chosen as models for glutamate and aspartate; acetamide and propanamide were chosen as models for glutamine and asparagine; ethylimidazole was chosen to model histidine; and dimethyl phosphate (DMP) was chosen as a generic model for phosphate. Since these test systems are very polar, they provide an appropriate test for the link atom approximation. Moreover, the division between QM and MM atoms is made next to a polar atom, which maximizes the effect of neglect of polarization in the MM region. In each case the results were compared with pure quantum calculations. The results are presented in Tables 4−8. The partitioning schemes are shown in Figure 2.

Carboxylates. Glutamate and aspartate are common ligands for metal ions in proteins. The interactions of these amino acids with Mg^{2+} and Ca^{2+} have been modeled by acetate and propanoate ligands. The minima of these complexes have C_{2v} symmetry with the carboxylates acting as bidentate ligands. Although there are examples of glutamate and aspartate acting as unidentate ligands to metals in proteins, only the bidentate complexes were studied here. The interactions in these complexes are very strong due to the attractive nature of the charged species, and the distances between the metals and carboxylates are very short. The HF−MM/DF−MM calculations accurately reproduce the energetics and structural features of the pure quantum calculations, and the Mulliken charges agree well (Figure 3 (I and II)).

TABLE 4: Binding Energies, ΔE in kcal mol^{-1} for Mg^{2+} and Ca^{2+} Complexes with Selected Ligands[a]

	acetate		propanoate	
	Mg^{2+}	Ca^{2+}	Mg^{2+}	Ca^{2+}
HF−MM	−387.29	−306.13	−383.04	−307.63
LDA−MM	−405.52	−314.23	−405.11	−313.68
BLYP−MM	−403.21	−310.44	−402.86	−310.02
HF	−387.15	−309.07	−384.17	−308.11
LDA	−407.98	−322.13	−406.17	−318.69
BLYP	−404.10	−318.52	−403.00	−315.79
MM	−333.44	−259.29	−337.58	−261.31
	acetamide		propanamide	
	Mg^{2+}	Ca^{2+}	Mg^{2+}	Ca^{2+}
HF−MM	−134.26	−90.30	−134.49	−94.03
LDA−MM	−141.77	−89.63	−146.50	−90.88
BLYP−MM	−139.74	−89.66	−131.36	−89.47
HF	−136.95	−91.20	−138.05	−94.09
LDA	−147.36	−92.24	−151.98	−94.08
BLYP	−144.33	−89.95	−148.89	−92.80
MM	−87.21	−62.92	−87.30	−63.03
	ethylimidazole		DMP	
	Mg^{2+}	Ca^{2+}	Mg^{2+}	Ca^{2+}
HF−MM	−138.33	−89.39	−387.32	−299.11
LDA−MM	−152.27	−88.61	−399.88	−299.61
BLYP−MM	−150.08	−88.41	−392.16	−298.75
HF	−140.31	−89.13	−379.11	−298.36
LDA	−156.68	−89.14	−401.79	−300.20
BLYP	−155.25	−90.43	−396.24	−302.77
MM	−102.41	−69.04	−307.18	−220.43

[a] A 6-31G* basis set was used for the quantum region with the exception of Ca, which had a TZV2P basis set of the Dunning type[68] [8s4p2d]^{rm}.[69] No counterpoise correction was used in the QM calculations.

TABLE 5: Structural Data for the Complexes of Acetate and Propanoate with the Mg^{2+} and Ca^{2+} Ions[a]

	acetate			propanoate		
	d(M−O)	∠MOC	d(C−O)	d(M−O)	∠MOC	d(C−O)
			Mg^{2+}			
HF−MM	1.922	86.57	1.251	1.935	86.57	1.255
LDA−MM	1.987	85.10	1.270	1.971	84.92	1.275
BLYP−MM	1.936	87.07	1.258	1.908	87.24	1.249
HF	1.919	87.54	1.267	1.903	87.69	1.265
LDA	1.945	85.71	1.290	1.926	85.56	1.287
BLYP	1.977	85.87	1.306	1.968	86.40	1.309
MM	1.831	89.59	1.266	1.827	91.53	1.280
			Ca^{2+}			
HF−MM	2.304	91.38	1.246	2.302	91.34	1.248
LDA−MM	2.275	88.43	1.266	2.270	89.97	1.284
BLYP−MM	2.321	88.91	1.282	2.284	90.18	1.299
HF	2.212	89.31	1.251	2.287	92.40	1.260
LDA	2.228	89.77	1.285	2.226	89.66	1.286
BLYP	2.287	90.00	1.300	2.280	90.05	1.300
MM	2.303	94.43	1.265	2.297	95.73	1.265

[a] A 6-31G* basis set was used for the quantum region with the exception of Ca, which had a TZV2P basis set of the Dunning type[68] [8s4p2d].[69] Bond distances are in Ångstroms, and angles are in degrees. Refer to Figure 2 for a depiction of the structure. No counterpoise method was used in the QM calculations.

TABLE 6: Structural Data for the Complexes of Acetamide and Propanamide with the Mg^{2+} and Ca^{2+} Ions[a]

	acetamide				propanamide			
	d(M−O)	∠MOC	*d*(C−O)	*d*(C−N)	*d*(M−O)	∠MOC	*d*(C−O)	*d*(C−N)
				Mg^{2+}				
HF−MM	1.794	169.60	1.268	1.280	1.802	169.77	1.273	1.283
LDA−MM	1.806	169.84	1.263	1.277	1.793	168.66	1.287	1.299
BLYP−MM	1.803	173.55	1.265	1.280	1.822	162.30	1.303	1.311
HF	1.781	171.00	1.278	1.288	1.781	171.30	1.284	1.286
LDA	1.788	161.60	1.301	1.305	1.785	161.48	1.302	1.302
BLYP	1.812	160.76	1.321	1.319	1.796	162.48	1.308	1.305
MM	1.869	175.4	1.252	1.347	1.869	174.7	1.253	1.348
				Ca^{2+}				
HF−MM	2.207	171.00	1.248	1.237	2.199	170.70	1.252	1.297
LDA−MM	2.132	171.95	1.270	1.309	2.130	166.58	1.272	1.308
BLYP−MM	2.193	170.99	1.251	1.238	2.170	166.75	1.287	1.322
HF	2.159	173.44	1.260	1.299	2.187	173.70	1.258	1.302
LDA	2.120	171.09	1.279	1.311	2.115	172.19	1.280	1.308
BLYP	2.173	171.52	1.293	1.324	2.149	172.70	1.300	1.328
MM	2.368	173.9	1.247	1.348	2.367	173.9	1.247	1.349

[a] A 6-31G* basis set was used for the quantum region with the exception of Ca which had a TZV2P basis set of the Dunning type[68] [8s4p2d].[69] Bond distances are in Å and angles are in degrees. Refer to Figure 2 for a depiction of the structure. No counterpoise correction was used in the QM calculations.

TABLE 7: Structural Data for the Complexes between Ethylimidazole and the Mg^{2+} and Ca^{2+} Ions[a]

	d(M−N)	∠MNC′ [b]	∠MNC″ [b]
		Mg^{2+}	
HF−MM	1.958	123.2	131.10
LDA−MM	1.958	122.6	128.70
BLYP−MM	1.987	124.1	128.90
HF	1.937	122.90	131.60
LDA	1.948	124.57	127.99
BLYP	1.979	107.00	127.80
MM	1.963	125.1	131.8
		Ca^{2+}	
HF−MM	2.403	122.60	132.00
LDA−MM	2.311	121.09	133.01
BLYP−MM	2.362	121.37	132.93
HF	2.376	117.80	137.10
LDA	2.304	120.09	133.73
BLYP	2.358	122.58	131.88
MM	2.492	124.6	131.9

[a] A 6-31G* basis set was used for the quantum region with the exception of Ca which had a TZV2P basis set of the Dunning type[68] [8s4p2d].[69] Bond distances are in Ångstroms, and angles are in degrees. [b] MNC′ refers to the angle made by the metal, nitrogen, and the carbon that is not bonded to the NH group. MNC″ refers to the angle with the carbon bonded to the NH group. Refer to Figure 2. No counterpoise correction was used in the QM calculations.

TABLE 8: Structural Data for the Complexes between DMP and the Mg^{2+} and Ca^{2+} Ions[a]

	d(M−O)	∠MOP	*d*(P−O)
		Mg^{2+}	
HF−MM	1.903	91.20	1.534
LDA−MM	1.919	88.63	1.540
BLYP−MM	1.951	88.79	1.591
HF	1.904	90.63	1.537
LDA	1.909	88.34	1.597
BLYP	1.935	88.47	1.597
MM	1.838	97.29	1.489
		Ca^{2+}	
HF−MM	2.300	96.10	1.528
LDA−MM	2.251	92.11	1.547
BLYP−MM	2.265	96.41	1.550
HF	2.285	95.88	1.522
LDA	2.217	92.03	1.544
BLYP	2.266	92.25	1.568
MM	2.335	100.80	1.486

[a] A 6-31G* basis set was used for the quantum region with the exception of Ca which had a TZV2P basis set of the Dunning type[68] [8s4p2d].[69] Bond distances are in Å and angles are in degrees. Refer to Figure 1 for a depiction of the structure. No counterpoise correction was used in the QM calculations.

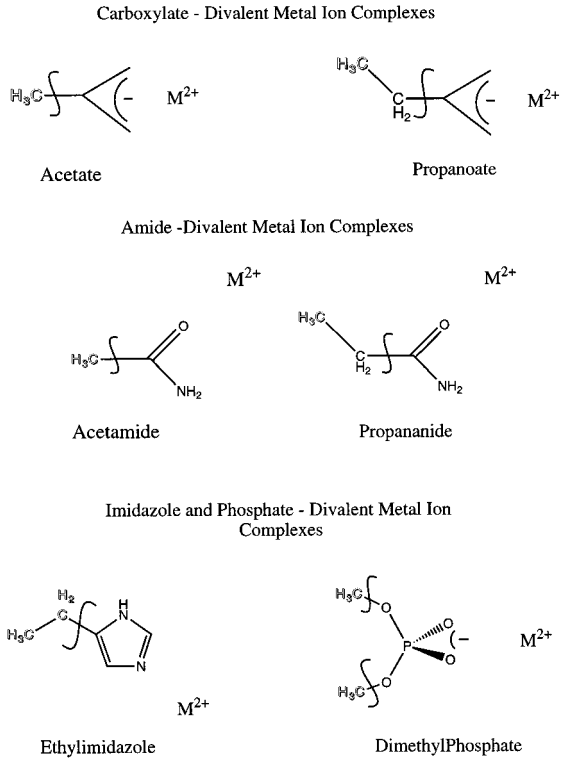

Figure 2. Partition schemes for the complexes of the cations M^{2+} with selected ligands. Ghosted atoms are in the classical region.

Amides. Both the acetamide and propanamide metal complexes serve as models for possible carbonyl−metal ion interactions found in the active sites of metalloenzymes involved in peptide hydrolysis.[64] The QM−MM results are in excellent agreement with pure quantum results. For both Mg^{2+} and Ca^{2+} the metal has a strong interaction with the carbonyl oxygen. The metal ion lies off the carbonyl vector, away from the nitrogen, consistent with the pure QM calculations. The binding energies of the amide complexes are larger than the corresponding complexes with water. This can be attributed to the greater polarizability of the carbonyl group. Figure 3 (III and IV) shows the Mulliken charges for these complexes. The agreement with pure quantum calculations is excellent, especially for those atoms further from the boundary between the quantum and classical regions.

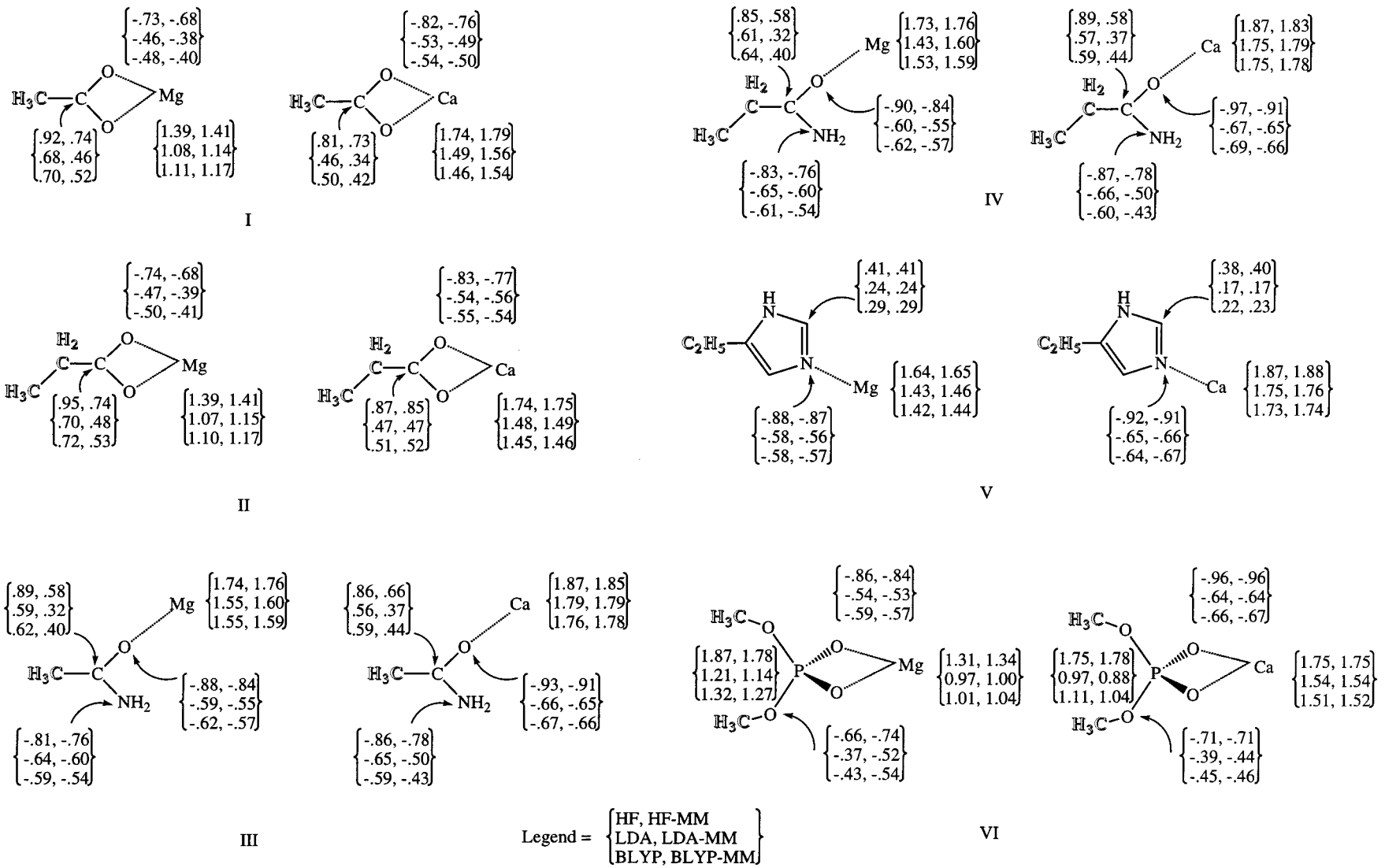

Figure 3. Mulliken charges for the model complexes with magnesium and calcium. For each atom the QM and QM−MM charges are shown in pairs for the HF, LDA, and BLYP Hamiltonians. (I)−(II) are the carboxylate complexes; (III) and (IV) are the amide complexes; (V) and (VI) are the imidazole complexes; (VII) and (VII) are the dimethyl phosphate complexes. Groups that were in the classical region in QM−MM calculations are ghosted.

Ethylimidazole. Histidine is another common ligand for metals in proteins. This amino acid was modeled by ethylimidazole. Since it is unwise to partition a molecule across a π-system,[8] the imidazole group is in the quantum region and the ethyl group in the classical region. The metal ions are positioned along the nitrogen lone pair vector and the binding energies for both ions are similar to those found for the complexes with amides. This QM−MM complex gives excellent agreement with pure quantum calculations. This is not unexpected since the boundary between the quantum and classical regions is far from the metal binding site. Again the Mulliken charges agree well (Figure 3 (V)).

DMP. Mg^{2+} and Ca^{2+} ions are known to form complexes with DNA and RNA and are known to have important roles in RNA folding and tertiary structure.[65] In recent years it has been found that dications act as cofactors for RNA cleavage reactions in ribozymes.[63] Dications have several possible binding sites on nucleotides, but we have chosen only to consider the one between these ions and the phosphate group. These complexes illustrate an advantage of the HF−MM/DF−MM potentials over MNDO-based QM−MM potentials since there are well-documented problems associated with using AM1 to study phosphorus-based compounds.[29] Like the carboxylates the interactions between the metals and DMP is very strong with a short metal−phosphate distance. The minima have C_{2v} symmetry. The HF−MM/DF−MM structural, energetic, and charge distribution results (Figure 3 (VI)) are very similar to the pure quantum results.

V. Timings

An important aspect of QM−MM calculations with different QM methods concerns the savings in computer time relative to full QM calculations. The execution time (cpu) for a single point calculation of the complex of ethylimidazole to magnesium is reduced from 19.12 to 7.52 s at the HF−MM level. For the complex of propanamide to calcium the execution time is reduced from 27.81 to 11.24 s at the LDA−MM level. In both cases the execution time is reduced by 50% with even a small part of the complex in the MM region (see Figure 2). For larger MM regions, the saving in time versus a full QM calculation could obviously be much more important.

VI. Conclusions

The study of simple binary complexes demonstrates that large improvements in the results for the QM−MM calculations are obtained by using Hartree−Fock or density functional methods for the quantum region instead of the semiempirical AM1 Hamiltonian. The largest improvement is found for the binding energies, but there is also an increase in the accuracy of the calculated geometries. The results are such that the method can be applied with some confidence to study reactions in biomolecules. However, in each case specific comparisons between QM and QM−MM calculations should be made to verify the approach for the system of interest.

The results with the link atoms are particularly encouraging. In some cases the partitioning scheme (e.g., for the complexes involving ethylimidazole and DMP) results in an essentially QM calculation with a perturbation from a distant alkyl group. However, these are exactly the types of partitioning that will be employed in simulations of the condensed phase chemistry of proteins and nucleic acids. The link atom is not the only approach available, but in the present cases it performs well. Other approaches have been used, most notably the frozen orbital method of Rivail and co-workers.[58]

Several methods have been reported in the literature for realizing linear scaling quantum calculations (HF and DF based). It is now possible to do approximate QM calculations for very large systems by the use of linear scaling methods.[66,67] However, the time required is such that semiempirical Hamiltonians are currently the only realistic methods available. Moreover, in most cases (other than electron transfer, for example) a full QM treatment is not necessary. Given the timing advantage from using QM−MM methods, as compared with pure QM calculations, and the level of accuracy that can be achieved based on the test cases presented here, we conclude that both HF−MM and DF−MM methods are a useful option for the accurate study of condensed phase chemistry, in general, and biomolecules in particular.

Acknowledgment. The Human Frontiers in Science Foundation is thanked for a fellowship to P.D.L. This work was supported in part by a grant from the National Science Foundation (M.K.). We are grateful to Dr. Nick Handy and Dr. R. D. Amos for providing us with a copy of the CADPAC code. The CHARMM program is available from the CHARMM Development Program, Department of Chemistry, Harvard University, and CADPAC is available from Prof. Nick Handy, University Chemical Laboratory, Lensfield Road, CB2 1EW, U.K. The GAMESS program can be obtained from Mike Schmidt (mike@si.fi.ameslab.gov). We thank the National Aeronautic and Space Agency for computer time.

References and Notes

(1) Szabo, A.; Ostlund, N. S. *Modern Quantum Chemistry*; McGraw-Hill: New York, 1989.
(2) Hehre, W. J.; Radom, L.; v. R. Schleyer, P.; Pople, J. A. *Ab Initio Molecular Orbital Theory*; Wiley: New York, 1986.
(3) Parr, R. G.; Yang, W. *Density functional theory of atoms and molecules*; Oxford University Press: New York, 1989.
(4) Head-Gordon, M. *J. Phys. Chem.* **1996**, *100*, 13213−13225.
(5) Warshel, A.; Levitt, M. *J. Mol. Biol.* **1976**, *103*, 227−249.
(6) Singh, U. C.; Kollman, P. A. *J. Comput. Chem.* **1986**, *7*, 718−730.
(7) Brooks, C. L.; Karplus, M.; Pettitt, B. M. *Proteins: A theoretical perspective of dynamics, structure, and thermodynamics*; New York, 1988.
(8) Field, M. J.; Bash, P. A.; Karplus, M. *J. Comput. Chem.* **1990**, *11*, 700−733.
(9) Thole, B.; van Duijnen, P. T. *Biophys. Chem.* **1983**, *18*, 53−59.
(10) Gao, J. L.; Xia, X. F. *Science* **1992**, *258*, 631−635.
(11) Stanton, R. V.; Hartsough, D. S.; Merz, K. M. *J. Comput. Chem.* **1995**, *16*, 113−128.
(12) Thery, V.; Rinaldi, D.; Rivail, J.-L.; Maigret, B.; Frenczy, G. G. *J. Comput. Chem.* **1994**, *15*, 269−282.
(13) Tunon, I.; Martins-Costa, M. T. C.; Millot, C.; Ruiz-Lopez, M. F.; Rivail, J. L. *J. Comput. Chem.* **1996**, *17*, 19−29.
(14) Maseras, F.; Morokuma, K. *J. Comput. Chem.* **1995**, *16*, 1170−1179.
(15) Thompson, M. A. *J. Phys. Chem.* **1995**, *99*, 4794−4804.
(16) Warshel, A. *Computer Modeling of Chemical Reactions in Enzymes and Solutions*; Wiley: New York, 1991.
(17) Harrison, M.; Burton, N.; Hillier, I. *J. Am. Chem. Soc.* **1997**, *119*, 12285−12291.
(18) Lee, Y.; Hodoscek, M.; Brooks, B.; Kador, P. *Biophys. Chem.* **1998**, *70*, 203−216.
(19) Dewar, M. J. S.; Zoebisch, E. G.; Healy, E. A.; Stewart, J. J. P. *J. Am. Chem. Soc.* **1985**, *107*, 3902.
(20) Gao, J. L. *J. Phys. Chem* **1992**, *96*, 537−540.
(21) Gao, J. *J. Am. Chem. Soc.* **1994**, *116*, 9324.
(22) Liu, H.; Muller-Plathe, F.; van Gunsteren, W. F. *J. Chem. Phys.* **1995**, *102*, 1722−1730.
(23) Liu, H.; Shi, Y. *J. Comput. Chem.* **1994**, *15*, 1311−1318.
(24) Bash, P. A.; Field, M. J.; Davenport, R. C.; Petsko, G. A.; Ringe, D.; Karplus, M. *Biochemistry* **1991**, *30*, 5826−5832.
(25) Lyne, P. D.; Mulholland, A. J.; Richards, W. G. *J. Am. Chem. Soc.* **1995**, *117*, 11345−11350.
(26) Elcock, A. H. E.; Lyne, P. D.; Mulholland, A. J.; Nandra, A.; Richards, W. G. *J. Am. Chem. Soc.* **1995**, *117*, 4706−4707.
(27) Stewart, J. J. P. *MOPAC 93.00 Manual*; Fujitsu Ltd.: Tokyo, 1993.

(28) Stewart, J. J. P. *J. Computer-Aided Mol. Design* **1990**, *4*, 1−105.
(29) Rzepa, H. S.; Yi, M. *J. Chem. Soc., Perkin Trans. 2* **1990**, 943−951.
(30) Jurema, M. W.; Shields, G. C. *J. Comput. Chem.* **1993**, *14*, 89−104.
(31) Stanton, R. V.; Little, L. R.; Merz, K. M. *J. Phys. Chem.* **1995**, *99*, 17344−17348.
(32) Wei, D.; Salahub, D. R. *Chem. Phys. Lett.* **1994**, *224*, 291−296.
(33) Kohn, W.; Sham, L. J. *Phys. Rev. A* **1965**, *140*, 1133−1138.
(34) Brooks, B. R.; Bruccoleri, R. E.; Olafson, B. D.; States, D. J.; Swaminathan, S.; Karplus, M. *J. Comput. Chem.* **1983**, *4*, 187−211.
(35) Cadpac 6.0: The Cambridge analytic derivatives package issue 6. Amos, R. D.; Albert, I. L.; Andrews, J. S.; Colwell, S. M.; Handy, N. C.; Jayatilaka, D.; Knowles, P. J.; Kobayashi, R.; Laidig, K. E.; Laming, G.; Lee, A. M.; Maslen, P. E.; Murray, C. W.; Rice, J. E.; Simandiras, E. D.; Stone, A. J.; Su, M.-D.; Tozer, D. J.; Cambridge University: Cambridge, U.K., 1995.
(36) Schmidt, M. W.; Baldridge, K. K.; Boatz, J. A.; Elbert, S. T.; Gordon, M. S.; Jensen, J. J.; Koseki, S.; Matsunaga, N.; Nguyen, K. A.; Su, S.; Windus, T. L.; Dupuis, M.; Montgomery, J. A. *J. Comput. Chem.* **1993**, *14*, 1347−1363.
(37) Vosko, S. H.; Wilk, L.; Nusair, M. *Can. J. Phys.* **1980**, *58*, 1200−1211.
(38) Ceperley, D. M.; Alder, B. J. *Phys. Rev. Lett.* **1980**, *45*, 566−569.
(39) Becke, A. D. *Phys. Rev. A* **1988**, *38*, 3098−3100.
(40) Lee, C.; Yang, W.; Parr, R. G. *Phys. Rev. B* **1988**, *37*, 785−789.
(41) Miehlich, B.; Savin, A.; Stoll, H.; Preuss, H. *Chem. Phys. Lett.* **1989**, *157*, 200−206.
(42) Murray, C. W.; Handy, N. C.; Laming, G. J. *Mol. Phys.* **1993**, *78*, 997−1014.
(43) Mackrell, A.; Bashford, D.; Bellot, M.; Dunbrack, R.; Evanseck, J.; Field, M.; Fischer, S.; Gao, J.; Guo, H.; Ha, S.; Joseph-McCarthy, D.; Kuchnir, L.; Kuczera, K.; Lau, F.; Mattos, C.; Michnick, S.; Ngo, T.; Nguyen, D.; Prodhom, B.; Reiher, W.; Roux, B.; Schlenkrich, M.; Smith, J.; Stote, R.; Straub, J.; Watanabe, M.; Wiorkiewicz-Kuczera, J.; Yin, D.; Karplus, M. *J. Phys. Chem.* **1998**, *102*, 3586−3616.
(44) Freindorf, M.; Gao, J. *J. Comput. Chem.* **1996**, *17*, 386−395.
(45) Roux, B.; Karplus, M. *J. Comput. Chem.* **1995**, *16*, 690−704.
(46) Jorgensen, W. L.; Chandrasekhar, J.; Madura, J. D.; Impey, R. W.; Klein, M. L. *J. Chem. Phys.* **1983**, 926−935.
(47) Neria, E.; Fischer, S.; Karplus, M. *J. Chem. Phys.* ***1996***, *105*, 1902−1921.
(48) Bleiber, A.; Sauer, J. *Chem. Phys. Lett.* **1995**, *238*, 243−252.
(49) Curtis, L. A.; Frurip, D. J.; Blander, M. *J. Chem. Phys.* **1979**, *71*, 2703−2711.
(50) Odutola, J. A.; Dyke, T. R. *J. Chem. Phys.* **1980**, *72*, 5062−5066.
(51) Foresman, J. B.; Brooks, C. L. *J. Chem. Phys.* **1987**, *87*, 5892−5894.
(52) Gao, J.; Garner, D. S.; Jorgensen, W. L. *J. Am. Chem. Soc.* **1986**, *108*, 4784−4790.
(53) Yamdagni, R.; Kebarle, P. *J. Am. Chem. Soc.* **1971**, *93*, 7139−7143.
(54) Ziegler, T. *Chem. Rev.* **1991**, *91*, 651.
(55) Gao, J. L. *J. Comput. Chem.* **1997**, *18*, 1061−1071.
(56) Thompson, M. *J. Phys. Chem.* **1996**, *100*, 14492−14507.
(57) Ho, L.; A. D. MacKerell, J.; Bash, P. *J. Phys. Chem.* **1996**, *100*, 4466−4475.
(58) Monard, G.; Loos, M.: Thery, V.; Baka, K.; Rivail, J.-L. *Int. J. quantum Chem.* **1996**, *58*, 153−159.
(59) Christoffersen, R. E.; Maggiora, G. M. *Chem. Phys. Lett.* **1969**, *3*, 419−423.
(60) Davis, T. D.; Maggiora, G. M.; Christofersen, R. E. *J. Am. Chem. Soc.* ***1974***, *96*, 7878−7887.
(61) Allen, L. C. *Ann. N. Y. Acad. Sci.* **1981**, *367*, 383−406.
(62) Lavie, A.; Allen, K. N.; Petsko, G. A.; Ringe, D. *Biochemistry* **1994**, *33*, 5469−5480.
(63) Wilcox, D. E. *Chem. Rev.* **1996**, *96*, 2435−2458.
(64) Pyle, A. M. *Science* **1993**, 709−714.
(65) Pyle, A. M.; Green, J. B. *Curr. Opinion Struct. Biol.* **1995**, *5*, 303−310.
(66) Burant, J. C.; Strain, M. C.; Scuseria, G. E.; Frisch, M. J. *Chem. Phys. Lett.* **1996**, *248*, 43−49.
(67) White, C. A.; Johnson, B. G.; Gill, P. M. W.; Head-Gordon, M. *Chem. Phys. Lett.* **1996**, *253*, 268−278.
(68) Dunning, T. H. *J. Chem. Phys.* **1971**, *55*, 716−723.
(69) McClean, A. D. *J. Chem. Phys.* **1980**, *72*, 5639−5648.